# Petrophysical Analysis and Seismic Attribute for Reservoir Characterization in "AMN"

# Field, Talang Akar Formation, South Sumatra Basin

**M. Alghiffari Ayman [1,a], Sudarmaji [1,b,*], and Muhammad Destrayuda Trisna [2,c]**

[1] Geophysics, Faculty of Mathematics and Natural Sciences, Universitas Gadjah Mada

Sekip Utara, Bulaksumur, Yogyakarta 55281, Indonesia

[2] Pertamina Hulu Rokan Zona 4 Prabumulih

Jalan Jenderal Sudirman No 03, Prabumulih 31113, Indonesia


e-mail: [a] aymandescend@mail.ugm.ac.id, [b] ajisaroji@ugm.ac.id, and [c] destrayudatrisna@gmail.com

\* Corresponding Author

## Abstract

The AMN field is located in the South Sumatra Basin, where the Talang Akar Formation is proven to be one of the main hydrocarbon reservoirs in the South Sumatra Basin, with the dominant lithology comprising interbedded sandstone and shale. This study aims to determine the depth and distribution of the reservoirs in the Talang Akar Formation using petrophysical analysis and seismic interpretation. Petrophysical analysis was performed using deterministic methods to obtain reservoir depth information vertically. The seismic interpretation was carried out using model-based acoustic impedance inversion and the application of the rms Amplitude attribute to get information on the lateral distribution of the reservoir. The result of petrophysical analysis indicated that the physical parameters in the AMN Field's Talang Akar Formation reservoir zone varied in depth, ranging from 1171.8 m to 1201.5 m, with an average shale content of 30%, water saturation of 70%, and effective porosity value of 15%. Seismic interpretation revealed the lateral distribution of sandstone reservoirs predominantly trending west to south in the study area, indicated by amplitude values ranging from 6,000 to 9,000 and acoustic impedance values from 6,400 to 7,200 (m/s)(g/cc). From this study, integrating petrophysical analysis using deterministic methods, model-based acoustic impedance inversion, and rms Amplitude attribute could provide reservoir distribution information both vertically and laterally.

**Keywords**: Petrophysical analysis; seismic interpretation; deterministic; model-based inversion; rms amplitude

## INTRODUCTION

The South Sumatra Basin is a Tertiary basin that has the potential to store hydrocarbon reserves [1]. The research targets the Talang Akar Formation (TAF), the main reservoir in the South Sumatra Basin. This formation was chosen based on its history of production in the research structure, where the primary oil producer is in the Talang Akar formation. The formation comprises coarse to fine-grained sandstone lithologies interspersed with shale and coal [2].
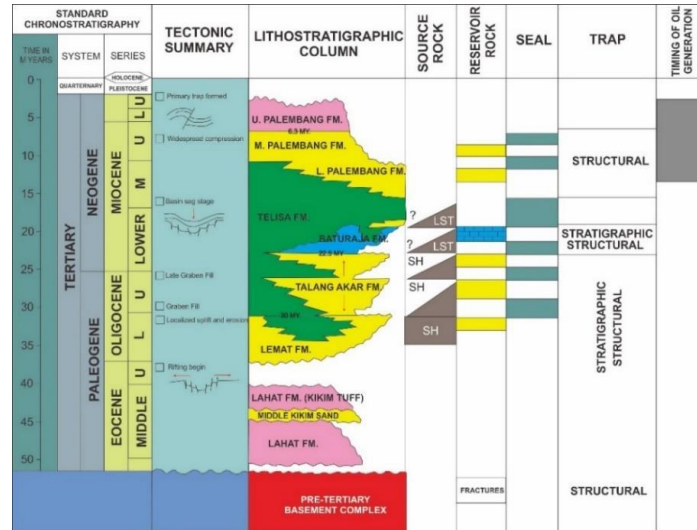


**Figure 1.** Stratigraphic of South Sumatra Basin [3]

Figure 1 shows the South Sumatra basin's stratigraphic column, composed of basements and formations formed during the transgression and regression phases. The transgression phase produced the Lahat, Lemat, Talang Akar, Baturaja, and Gumai Formations. Meanwhile, the regression phase caused the formation of the Air Benakat Formation, Muara Enim, Kasai, and Alluvial Deposits [3,4].

Before the discovery of modern exploration methods, exploration for positioning wells was only determined based on geological structure information, but not necessarily a geological structure containing an economical amount of hydrocarbons [5]. As technology develops, more accurate methods are used in hydrocarbon exploration, namely seismic and petrophysical methods. The seismic method has an excellent horizontal resolution, while petrophysical analysis using well-logging data produces good vertical resolution. Combining these two methods will create a more accurate interpretation of the data to describe the subsurface reservoir's character.

In this study, we discuss a combination of methods for determining hydrocarbon locations both vertically using petrophysical analysis and horizontally using seismic methods. The use of petrophysical analysis in reservoir characterization has been applied by previous researchers, such as Gahana et al. [6], to obtain petrophysical parameter values, such as shale content, porosity, water saturation, and permeability, as well as identify potential zones as hydrocarbon reservoirs. Model-based acoustic impedance inversion was applied by Ginting et al. [7] to characterize the reservoir with a seismic inversion approach. The petrophysical analysis method used by Gahana et al. determined the location of zones with the potential for a vertical reservoir. Still, other methods were not used to determine their vertical distribution.

Meanwhile, Ginting et al.'s seismic inversion approach succeeded in determining the reservoir's lateral distribution but only used a cross plot to determine its vertical location. Both studies use methods that can only determine the reservoir's location in one direction. So, in this research, a combination of petrophysical analysis methods and seismic interpretation was carried out to characterize the reservoir horizontally and vertically.

Reservoir characterization is the process of studying all the characteristics of a reservoir related to its ability to store and produce hydrocarbons. In the reservoir characterization process, petrophysical analysis plays a role in determining the reservoir's physical parameters, including porosity, shale content, and water saturation [8]. Through these parameters, it can be seen at what depth some zones can potentially contain hydrocarbon reserves. Then, integration between log data and seismic data is carried out using seismic attributes and acoustic impedance inversion to produce information on subsurface geological appearance and reservoir distribution patterns in the target area.

## METHOD
### Data Source
The data used in this research is the property of PT Pertamina Hulu Rokan Zone 4, which consists of three deviation wells with the initials AMN-32, AMN-33, and AMN-44. The data of three wells consist of well-log, mud-log, well report, checkshot data, and 3D seismic data. Well-log data consists of gamma ray log, caliper, spontaneous potential, resistivity, neutron, density, and sonic log. The seismic data used is 3D Post-Stack Time Migration seismic data with inline 1.050 - 1.200 and xline 10.300 - 10.650, with sampling intervals of 2 ms.

### Petrophysical Analysis
Petrophysical analysis was carried out using Microsoft Excel software and Interactive Petrophysics 4.5. The following are the petrophysical analysis steps carried out for research [8,9]:

#### Data Input
The research began by inputting data from 3 wells, as well as additional geological data and marker data. These data are the main data used for petrophysical analysis.

#### Precalculation
Initial calculations are carried out at this stage before conducting petrophysical analysis. The calculation includes calculating the actual vertical depth and the temperature change gradient along the borehole. The result of this stage is the actual depth value and the value of the borehole temperature gradient. The actual depth calculation needs to be done because the well used is a deviation well, so the measured depth value is different from the actual depth. Temperature gradient calculations are carried out to obtain information on changes in temperature along the borehole due to an increase in pressure with an increase in depth. The results of the temperature gradient calculation will affect the drilling mud, the resistivity of the mud filtrate, and the resistivity of the formation water.

#### Environmental Correction

Environmental correction is a process that aims to minimize the effect of the borehole and the type of logging tool used during the well logging process on the measurement results. The Schlumberger correction module is used as a logging services company, to carry out environmental corrections for the three wells used. The logs that will be corrected for reading results are in the form of gamma ray logs, density logs, and neutron logs.

Normalization

Data normalization is a process that aims to equalize the distribution of the log data used. This difference in distribution can occur due to differences in logging tools used and different measurement times. Data normalization was performed on the gamma ray log, using a reference well in the form of AMN-32. The result of normalization is a better distribution of values from the gamma ray log so that the gamma ray log can be better used for further analysis.

Badhole Identification

Identification of badholes aims to determine the zones that experience caving/washout and mudcake using caliper logs and drill bit size logs. When the caliper log value is lower than the log bitsize, mudcake is identified, which causes the diameter of the drill hole to decrease. However, if the caliper log value is higher than the log bitsize, it indicates caving/washout, which is a condition in which the diameter of the borehole increases due to the collapse of the drill wall.

Shale Content Calculation

Shale content (Vshale) is calculated to determine shale content along the depth interval of the well, which is divided into several zones. This process is carried out using the results of log gamma ray readings that have been corrected and normalized. A linear equation is used to calculate the shale content, in which the minimum and maximum log gamma ray values are used as input, as shown in the following equation [8,9]:

$$I_\gamma = \frac{\gamma_{log} - \gamma_{min}}{\gamma_{max} - \gamma_{min}} \tag{1}$$

where $I_\gamma$ is the gamma ray index, $\gamma_{log}$ is the gamma ray reading of formations, and $\gamma_{min}$, $\gamma_{max}$ are minimum and maximum value of gamma rays.

Porosity Calculation

Porosity is the ratio between the volume of empty space (pores) in a lithology to the total volume of the lithology [9]. Porosity calculations are carried out using the neutron-density equation, with inputs in the form of neutron log (NPHI) and density (RHOB). Neutron porosity measures the hydrogen atom content in the rock fluid, while density porosity measures the bulk density of the rock. The Bateman-Konen equation is used to calculate effective porosity, while the Wyllie-Rose equation is used to obtain density porosity [10]. The parameters for calculating the total shale porosity were obtained from the cross-plot between the neutron-density logs, as shown in Figure 2.

$$\Phi_E = \frac{\Phi_D \times \Phi_{N_{sh}} - \Phi_N \times \Phi_{D_{sh}}}{\Phi_{N_{sh}} - \Phi_{D_{sh}}} \tag{2}$$

$$\Phi_D = \frac{\rho_{MA} - \rho}{\rho_{MA} - \rho_W} - V_{sh}\left(\frac{\rho_{MA} - \rho_{sh}}{\rho_{MA} - \rho_W}\right) \tag{3}$$

$$\Phi_{T_{sh}} = \frac{\rho_{D_{sh}} - \rho_{sh}}{\rho_{D_{sh}} - \rho_W} \tag{4}$$

$$\Phi_T = \Phi_E + V_{sh} \times \Phi_{T_{sh}} \tag{5}$$

where $\Phi_E$ is the effective porosity, $\Phi_D$ is the density porosity, $\Phi_N$ is the neutron porosity, $\Phi_{T_{sh}}$ is the total shale porosity, $\Phi_T$ is the total porosity, $\Phi_{D_{sh}}$ is the density shale porosity, $\Phi_{N_{sh}}$ is the neutron shale porosity, $\rho_{MA}$ is the matriks density, $\rho_{sh}$ is the shale density, $\rho_{D_{sh}}$ is the dry shale density, and $\rho_W$ is the water density.

Water Saturation Calculation

Water saturation is the percentage of water volume that fills the pores in the rock. It is a physical parameter that can be used to determine hydrocarbon saturation in a reservoir because every rock pore must be filled with fluids, both hydrocarbons and water [9]. Calculation of water saturation is carried out using the Archie Equation for non-shaly formations and the Indonesian Equation for shaly formations [10,11].

$$S_{w_A} = \sqrt[n]{\frac{a R_w}{\Phi_e^m R_t}} \tag{6}$$

$$S_{w_I} = \left\{ \frac{\sqrt{\frac{1}{R_t}}}{\left(\frac{V_{sh}\left(1-\frac{V_{sh}}{2}\right)}{\sqrt{R_{sh}}} + \sqrt{\frac{\Phi_E^m}{a \times R_w}}\right)} \right\}^{\left(\frac{2}{n}\right)} \tag{7}$$

where $S_{w_A}$ is the Archie water saturation, $S_{w_I}$ is the Indonesia water saturation, $a$ is tortuosity factor, $m$ is the cementation factor, $n$ is the saturation factor, $R_t$ is true resistivity, $R_w$ is the formation water resistivity, $R_{sh}$ is the shale resistivity, and $V_{sh}$ is the shale volume.

Lumping

The lumping process presents the results of petrophysical analysis, resulting from applying the shale volume cut-off values, effective porosity, and water saturation. Determining the cut-off value is carried out interpretively, considering the company's production data. This process aims to find a reservoir and pay zone, which is a zone identified as a reservoir of a well that has the potential to contain hydrocarbons. A cut-off value of 50% is used for the shale content and 10% for the effective porosity. The application of cut-off values to water saturation aims to obtain information on the hydrocarbon saturation in the reservoir. The value of 70% is used as the water saturation cut-off value. Zones with shale content and water saturation values lower than the cut-off and effective porosity values higher than the cut-off are identified as net pay zones.

**Seismic Interpretation**

The seismic interpretation was done using 3D Post-Stack Time Migration seismic data,

using Hampson Russell 10.3 and Schlumberger Petrel 2017 as processing software. The following are the stages in seismic interpretation [12,13]:

Data Input

This study's seismic interpretation process begins by entering seismic data and marker data into the software, as well as additional geological data to assist interpretation. Log data is also needed in the form of sonic log (DT) and density log (RHOB), as well as checkshot data to make synthetic seismograms.

Checkshot Correction

Checkshot correction is a process of correcting sonic logs using checkshot data. Checkshot data is data obtained from the vertical seismic profiling process. The checkshot correction process is carried out to improve the accuracy of seismic wave velocity calculations, because the sonic log is susceptible to changes in borehole conditions, such as washouts. In contrast, the checkshot does not have a resolution as detailed as the sonic log [14].

Wavelet Extraction

Wavelet extraction is performed to obtain wavelets, which will be used for further analysis [14,15]. The extracted wavelet is a statistical wavelet with zero phase. Wavelets are extracted at a time window of 1,100 to 1,200 ms, with a length of 100 ms, a taper length of 25 ms, a sampling rate of 2 ms, and a phase of 0°.

Well Seismic Tie

Well seismic tie is the process of binding well data with a depth domain with seismic data with a time domain (two-way time). It aims to obtain a correlation between well data and seismic data, with at least a 60% correlation [15].

This process begins with creating synthetic seismograms from the corrected sonic log data and density logs convoluted with previously extracted wavelets. Furthermore, binding is carried out between traces on synthetic seismograms and traces from seismic by performing time shifting until a good correlation is obtained. The time windows used are focused on the target reservoir.

Horizon Picking

The picking process is one of the seismic section interpretation processes that aims to identify the targeted layer (horizon) that will be processed into a time structure map. The picking process is performed at 1,050 to 1,200 and xline 10,350 to 10,600, with increments of 5.

Attribut Extraction

The attribute extraction process is carried out to overlay the attributes used with the time structure map. The extracted attribute is the amplitude rms attribute, which is the result of calculating the average square root of the amplitude squares at a certain time interval. It is very sensitive to changes in the amplitude value, as in equation (8) [16].

$$A_{rms} = \sqrt{\frac{1}{N}\sum_{i=1}^{N} A_i^2} \qquad (8)$$

where $A_{rms}$ is the value of rms amplitude, $A$ is the value of seismic amplitude, and $N$ is the amplitude sample in the time window.

Seismic Inversion

Seismic inversion is a method of making a geological model from a seismic section to an acoustic impedance model, using seismic data, well data, and geological information as a controller. Seismic inversion aims to reduce the wavelet effect by modeling the acoustic impedance at certain time intervals, which can provide information on subsurface layers [17,18]. Inversion is carried out using a model-based method, which is an inversion method that uses iterations of forward modeling and a comparison between the results of the acoustic impedance model and the seismic trace, which will show the error value [19].

The process of acoustic impedance inversion begins with a sensitivity test, using a crossplot between sonic logs and density so that the distribution of lithology in the study area can be seen. Next, the initial model is made, which is the initial acoustic impedance volume model, which is obtained through a process using density data, acoustic impedance, sonic log, and the results of the horizon picking that has been done. This initial model will be used as a control for the resulting inversion model. This model uses the parameter high cut frequency 13 to 20 Hz, so frequencies that exceed that scale will be eliminated. To see the level of accuracy of the resulting initial model, a crossplot analysis was performed between the initial acoustic impedance log and the inverted acoustic impedance log.

Furthermore, an inversion analysis is performed on the model that has been made. This process begins by determining several parameters, such as block size, number of iterations, constraints, time windows, and prewhitening. The block size parameter is intended to set the block size resulting from the inversion according to the control of the seismic data and the initial model that has been made. The value of 2 ms is used for the average block size parameter. Moreover, the number of iterations parameter aims to obtain an optimal correlation between synthetic and actual seismic traces. The number of iterations is 10. The constraint parameter aims to regulate the modeling process, where the higher it is, the closer it is to the initial model, while the lower it is, the more it resembles a seismic trace. The soft constraint parameter of 0.5 is used to control the modeling. The time windows used are the top and bottom horizons, and for the prewhitening parameter (frequency filter to remove noise), a value of 1% is used. After obtaining a good correlation from the results of the inversion of the acoustic impedance log with the initial acoustic impedance log, it can be run to get the cross-sectional volume of the acoustic impedance inversion.

## RESULTS AND DISCUSSION
### Petrophysical Analysis

The petrophysical analysis produces physical parameter values in shale content, porosity, and water saturation. The results of these parameters will be used for the lumping process, namely determining the cut-off value to obtain the net pay zone. Physical parameters are calculated for each well by dividing it into several zones. The results of the calculations are presented in Tables 1, 2, and 3.

**Table 1.** Tabulation of the average values of Vshale, PHIE and Sw on AMN-32

| Well | Zone | Top TVD (m) | Bot TVD (m) | Avg Vshale | Avg PHIE | Avg Water Saturation |
|------|------|-------------|-------------|------------|----------|----------------------|
| AMN-32 | 2 | 244.81 | 430.02 | 62.27 | 12.21 | 89.78 |
| | 3 | 430.02 | 700.13 | 54.94 | 10.13 | 93.69 |
| | 4 | 700.13 | 839.51 | 43.38 | 21.79 | 90.76 |
| | 5 | 839.51 | 1007.94 | 60.21 | 11.38 | 86.48 |
| | 6 | 1007.94 | 1116.62 | 50.52 | 14.2 | 91.65 |
| | 7 | 1116.62 | 1253.33 | 48.94 | 6.21 | 94.18 |

**Table 2.** Tabulation of the average values of Vshale, PHIE and Sw on AMN-33

| Well | Zone | Top TVD (m) | Bot TVD (m) | Avg Vshale (%) | Avg PHIE (%) | Avg Water Saturation (%) |
|------|------|-------------|-------------|----------------|--------------|--------------------------|
| AMN-32 | 2 | 251.81 | 439.22 | 60.95 | 12.14 | 92.58 |
| | 3 | 439.22 | 701.31 | 65.01 | 10.43 | 93.74 |
| | 4 | 701.31 | 1026.34 | 55.46 | 8.82 | 96.5 |
| | 5 | 1026.34 | 1117.61 | 58.39 | 5.81 | 92.36 |
| | 6 | 1117.61 | 1161.52 | 65.12 | 3.98 | 64.3 |
| | 7 | 1161.52 | 1265.91 | 40.27 | 3.06 | 98.49 |

**Table 3.** Tabulation of the average values of Vshale, PHIE and Sw on AMN-44

| Well | Zone | Top TVD (m) | Bot TVD (m) | Avg Vshale (%) | Avg PHIE (%) | Avg Water Saturation (%) |
|------|------|-------------|-------------|----------------|--------------|--------------------------|
| AMN-44 | 2 | 598.12 | 743.51 | 70.08 | 8.3 | 95.46 |
| | 3 | 743.51 | 981.33 | 61.83 | 12.91 | 93.42 |
| | 5 | 1124.21 | 1213.94 | 59.33 | 6.04 | 90.67 |
| | 6 | 1213.94 | 1288.31 | 36.21 | 19.96 | 99.19 |

Tables 1, 2, and 3 show the average values of shale content, effective porosity values, and water saturation values of the zones in each well. By applying the cut-off to these results, information will be obtained on the net pay zone, which is a potential hydrocarbon zone. A cut-off value of 50% for shale content, 10% for effective porosity, and 70% for water saturation is used. The result of applying this cut-off value is net pay zone information and its physical parameters, as shown in Table 4.

**Table 4.** Tabulation of lumping results for the three wells

| Well | Zone | Top TVD (m) | Bot TVD (m) | Net Pay Interval (m) | Avg Vshale (%) | Avg PHIE (%) | Avg Water Saturation (%) |
|---|---|---|---|---|---|---|---|
| AMN -32 | A | 1171.8 | 1177.9 | 6.1 | 22.9 | 19.2 | 46.2 |
|  | B | 1180.9 | 1183.2 | 2.3 | 25.8 | 15.9 | 65.6 |
| AMN -33 | A | 1173.7 | 1177.4 | 3.7 | 16.5 | 17.3 | 50.2 |
|  | B | 1182.5 | 1185.7 | 3.2 | 16.9 | 19.9 | 57.2 |
| AMN -44 | A | 1186.3 | 1189.5 | 2.6 | 29.3 | 17.48 | 69.4 |
|  | B | 1199.6 | 1201.5 | 1.9 | 13.9 | 26 | 41.1 |

The lumping results shown in Table 4 show that two zones in each well are categorized as net pay zones. These zones are zones A and B. The net pay zone is in the Talang Akar Formation, which is the final result of the petrophysical analysis. Furthermore, through seismic interpretation, the distribution direction of the reservoir in net pay zones A and B will be obtained.

**Seismic Interpretation**

Seismic interpretation is carried out to obtain information on reservoir distribution in the net pay zone, using the application of the amplitude RMS attribute, and model-based acoustic impedance inversion. The results of the seismic interpretation are a time structure map, amplitude rms attribute maps, acoustic impedance inversion sections, and acoustic impedance inversion maps.

Time Structure Map

A time structure map is a map that provides a topographic visual of a horizon on a seismic section using the time domain (ms). It is made using the results of horizon picking to display the topography of that horizon [20]. The results of the time structure map can be seen in Figures 3 and 4.
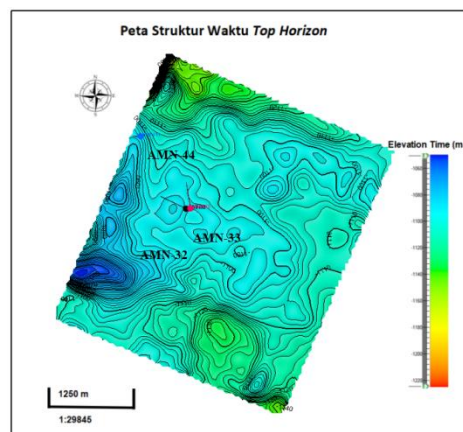


**Figure 3.** Top Horizon Time Structure Map
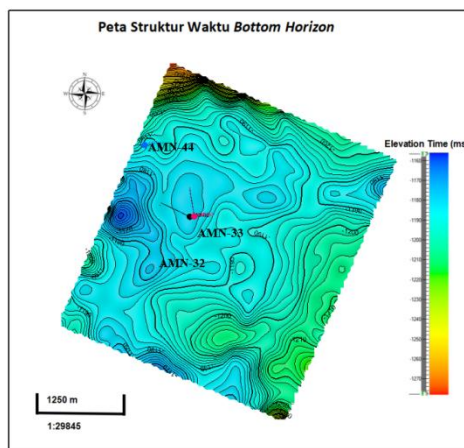
**Figure 4.** Bottom Horizon Time Structure Map

Figures 3 and 4 are the results of time structure maps for the top and bottom horizons. Figure 3 shows the top horizon, the upper boundary of the Talang Akar Formation, through which wells in the AMN field pass, while Figure 4 shows the bottom horizon, which is the upper boundary of the basement. Both maps show the dominance of blue color, indicating that the topography of the two horizons is relatively even.

The results of the top horizon time structure map show that the topographical interval is at -1,060 ms to 1,220 ms, while for the bot horizon it is at -1,160 ms to -1,270 ms. The top horizon time structure map shows the dominance of light blue topography, with a value of -1,100 ms, and there are elevations in the southwest part of the study area, with a value of -1,060 ms, and valleys in the north of the study area with a value of -1,200 ms. The bottom horizon time structure map shows the dominance of light blue topography, with a value of -1,190 ms, which is interpreted as an area that has a relatively flat elevation and there are elevations in the western and southern parts of the study area, with a value of -1,160 ms, and there are valleys in the north of the study area with a value of -1,270 ms.

The top horizon time structure map results show that the topographical interval is at -1,060 ms to 1,220 ms, while for the bot horizon, it is at -1,160 ms to -1,270 ms. The top horizon time structure map shows the dominance of light blue topography, with a value of -1,100 ms, and there are elevations in the southwest part of the study area, with a value of -1,060 ms, and valleys in the north of the study area with a value of -1,200 ms. The bottom horizon time structure map shows the dominance of light blue topography, with a value of -1,190 ms, which is interpreted as an area with a relatively flat elevation. There are elevations in the western and southern parts of the study area, with a value of -1,160 ms, and valleys in the north of the study area, with a value of -1,270 ms.

RMS Amplitude Map

The amplitude rms attribute map is generated by applying the attribute to a seismic cross-section layer sliced 50 ms below the top horizon. This is done because the target zone is 50 ms below the top horizon. The high amplitude rms value indicates the distribution of sandstone lithology [20]. Figure 5 is an amplitude rms map sliced 50 ms below the top horizon.
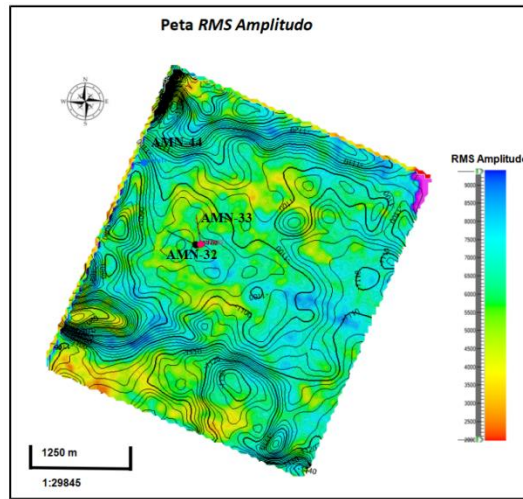
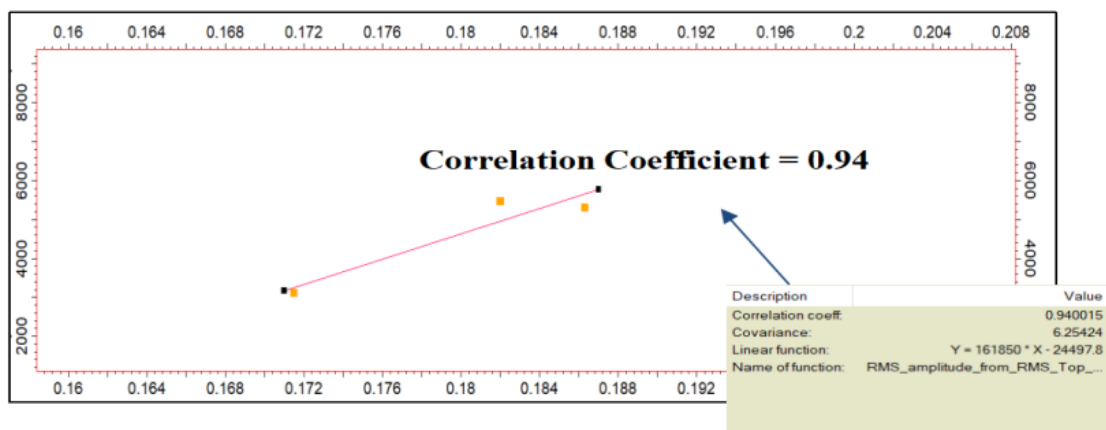**Figure 5.** RMS Amplitude Map



**Figure 6.** Crossplot PHIE (x) vs RMS Amplitud (y)

Figure 6 shows the crossplot between the effective porosity value and the rms amplitude value of each well, where a 94% correlation value is obtained, indicating that the amplitude rms attribute extraction results are quite good [20, 21]. The results of the amplitude rms map show that the range of rms amplitude values is in the interval 2,000 to 9,000. The distribution of sandstone lithology is indicated by blue areas with amplitude values of 6,000 to 9,000, which are spread from the center of the study area to the south.

Seismic Inversion

The process of acoustic impedance inversion begins with a sensitivity test, using a crossplot between sonic logs and density, so that the lithology distribution in the study area can be seen, as shown in Figure 7.
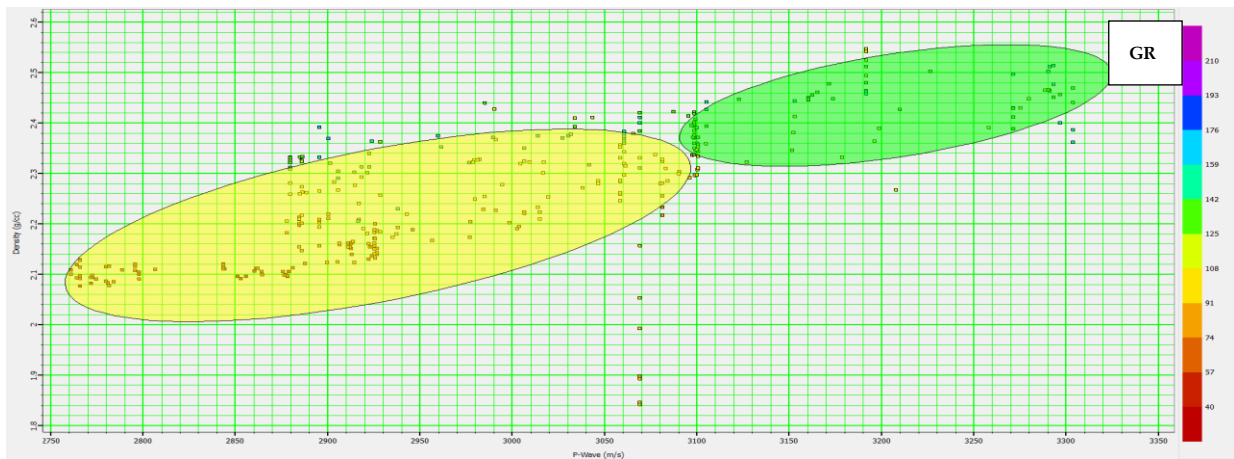
**Figure 7.** Sensitivity Test on AMN-32

Figure 7 is a sensitivity test in the AMN-32 well. The sensitivity test results showed a good distribution between sand (yellow circle) and shale (green circle) lithology, which allowed for the next step of analysis, namely making the initial model. The initial model shown in Figure 8, with a correlation of 59% between original and inverted acoustic impedance, shows a good correlation, as shown in Figure 9.

Figure 9 is a crossplot between the original acoustic impedance log and the inverted acoustic impedance log, which produces a correlation value of 59%. This correlation value indicates that the consistency and relationship between the inverted and original data are good enough for the initial model to be used for further processing [22]. Then, an inversion analysis was performed using the created model, as shown in Table 5.
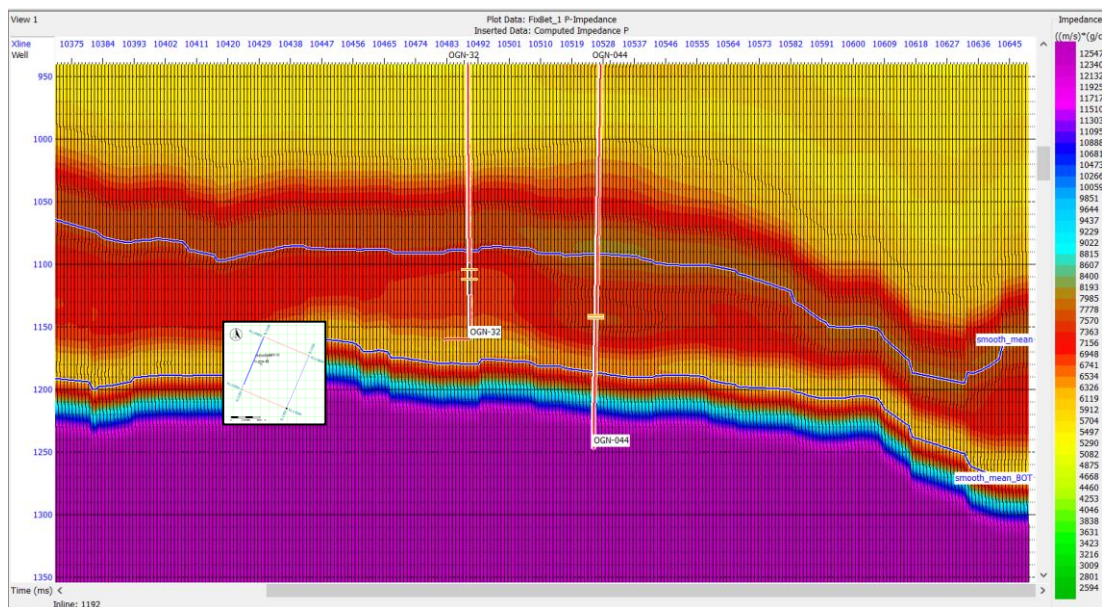


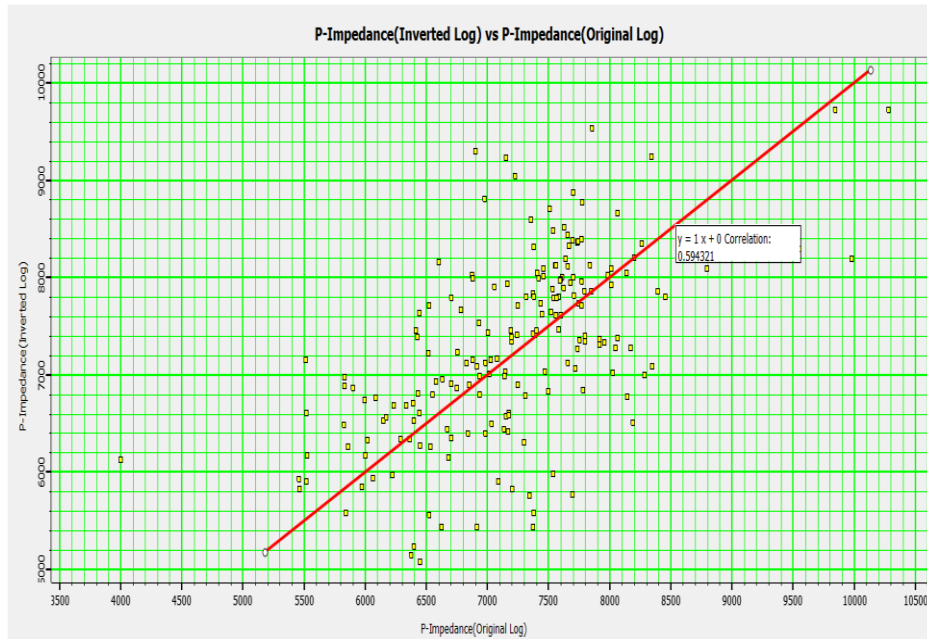**Figure 8.** Initial acoustic impedance model at Inline 1200

**Figure 9.** Initial acoustic impedance crossplot and inversion results

After obtaining a good correlation between the results of the acoustic impedance log inversion and the initial acoustic impedance log, the procedure can be run to obtain the cross-sectional volume of the acoustic impedance inversion. The results of the inversion are shown in Figure 10.

**Table 5.** Tabulation of inversion analysis result for the three wells

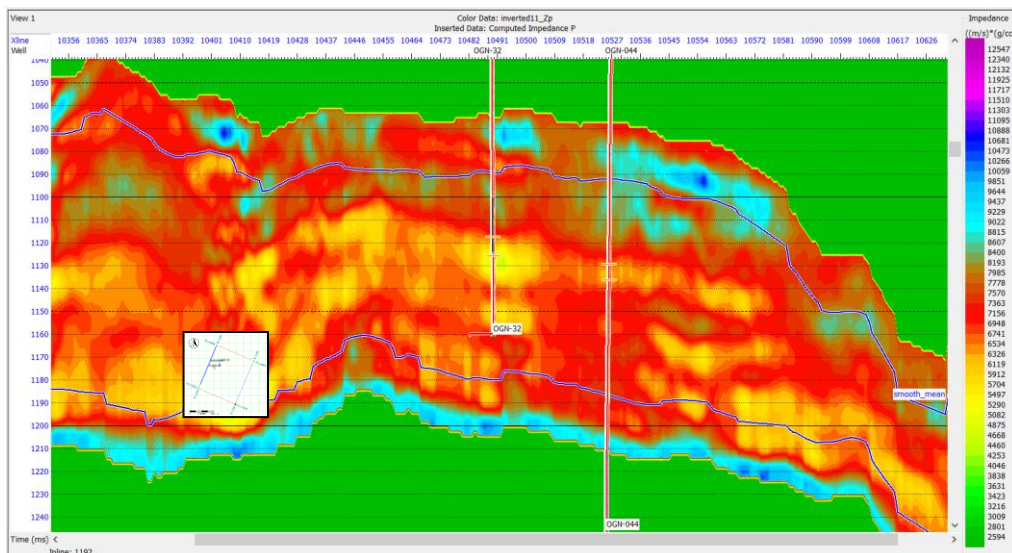| Well | Correlation (%) | Error (%) |
|---|---|---|
| AMN-32 | 98.9 | 19.5 |
| AMN-33 | 95.6 | 32.9 |
| AMN-44 | 93.3 | 47.4 |



**Figure 10.** Result of "AMN" field acoustic impedance inversion in Inline 1200

Acoustic impedance inversion results show lithological layering, with variations in acoustic impedance values ranging from 2,594 to 12,547 (m/s)(g/cc). Sandstone lithology has an acoustic impedance value below 7,200 (m/s)(g/cc); it is identified as shale above this value. Then, the acoustic impedance inversion results are overlaid with the time structure map, which is dissected 50 ms below the top horizon. This process is carried out to see the distribution of acoustic impedance values in the target.
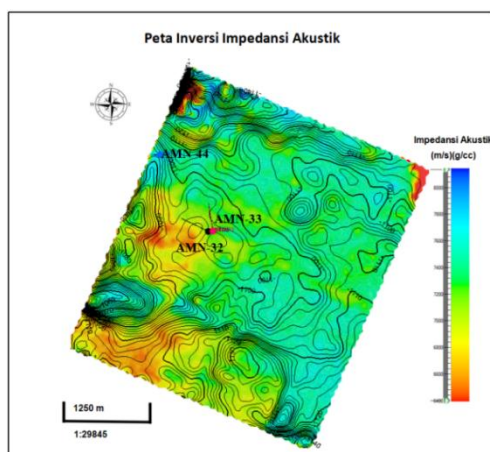


**Figure 11.** Acoustic impedance map that slices 50 ms below the top horizon

The map result in Figure 11 shows the distribution of acoustic impedance values with intervals of 6,400 to 8,000 (m/s)(g/cc) in the target area. The distribution of lower values is in the West to the South of the study area, with a predominance of yellow to red colors, indicating sandstone lithology [22, 23]. The results of the acoustic impedance map have a pattern similar to the amplitude RMS attribute map in Figure 4, namely the distribution towards the South, thereby validating the acoustic impedance inversion result map in the study area. The distribution pattern of the sandstone lithology is the final result of the seismic interpretation that has been carried out.

The results of the petrophysical analysis show that the net pay zone in the three wells belongs to the shaly sand zone, with good porosity and moderate water saturation. The porosity value is affected by the shale content, in which the higher the shale content, the lower the porosity value. In comparison, the water saturation value affects the hydrocarbon content in the rock porosity [24]. This is consistent with the results obtained in this study and previous studies using petrophysical analysis. The obtained petrophysical parameters provide information on the depth of the net pay zone, at which depth a seismic interpretation is carried out to obtain its distribution. By applying the RMS amplitude attribute, the amplitude change anomaly can be adequately observed so that the initial assumptions about the direction of the reservoir distribution can be known. This is because the RMS amplitude values in the reservoir and non-reservoir zones have contrasting values [25,26]. Furthermore, by inverting the acoustic impedance, the impedance value of the rock can be known and becomes excellent additional information to determine the directional distribution of the reservoir. By integrating the results of the RMS amplitude and seismic inversion, the lateral distribution of the reservoir can be identified.

The limitation of this research is the insufficient availability of data, such as Special and Routine Core Analysis, which can be used for probabilistic calculations and can calculate the

influence of other mineral content on rock formations [27]. The use of attributes limited to amplitude RMS and model-based acoustic impedance inversion methods also means that this study does not have a more complete comparison of inversion results and validation of attribute results. However, the petrophysical analysis method used in this study is deterministic, which does not consider the other mineral content contained in rock formations [28]. So it is recommended for future researchers to be able to use probabilistic methods in petrophysical analysis, which pay attention to the content of other minerals in rock formations, as well as use other seismic inversion methods to compare the best results such as sparse spike and band-limited method and apply several additional seismic attributes such as envelope and sweetness [29, 30].

## CONCLUSION

Petrophysical parameter values in the AMN Field Talang Akar Formation indicate reservoir potential, with an average value of shale content < 30%, water saturation value < 70%, and effective porosity value > 15%. These results indicate that the reservoir zone is relatively shaly sand with good porosity and moderate water saturation. The depth of the net pay zone is in a different range for each well, as shown in Table 4, which is obtained from the application of cut-off on petrophysical parameters. The net pay zone is interpreted using the RMS Amplitude attribute and acoustic impedance inversion. Crossplot analysis for the amplitude RMS attribute produces a high correlation, namely 0.94%, so it can be used as an initial assumption of the distribution of sandstone reservoirs. The results of the integration of the amplitude RMS attribute and acoustic impedance inversion show that the distribution of sandstone reservoirs is relatively towards the west to the south of the study area, with an interval of 6,400 to 7,200 (m/s)(g/cc) acoustic impedance values. The results of this study are expected to become recommendations for further drilling and become material for improvement for further research using more advanced methods, such as probabilistic analysis for petrophysics and other additional seismic attributes.

## ACKNOWLEDGMENT

## AUTHOR CONTRIBUTIONS

M. Alghiffari Ayman: Conceptualization, Methodology, Formal Analysis, Project Administration, Data Curation, and Writing - Original Draft; Sudarmaji: Conceptualization, Methodology, and Validation; Muhammad Destrayuda Trisna: Resources, Conceptualization, Methodology, and Validation.

## DECLARATION OF COMPETING INTEREST

The authors declare that they have no known competing financial interests or personal relationships that could have appeared to influence the work reported in this paper.

## REFERENCES

[1] Wibowo AW, et al. Basin Center Play; Evaluation and Recent Update as Alternative Play in South Sumatra Basin. *Proceedings of PIT IAGI 51st*; 2022. Available from: https://www.iagi.or.id/web/digital/71/PITIAGI-22-P-Abs-103.pdf.

[2] Pramudito, D, Nugroho D, and Abdurrachman M. Reservoir Characterization and Compartment in Postrift Deposited, Upper Talangakar Formation, Belut Field, South Sumatra Basin. *Bulletin of Geology.* 2021; **5**(2): 638-651. Available from: https://buletingeologi.com/index.php/buletin-geologi/article/view/106.

[3] Toha MT, Setiabudidaya D, Ghadafi MA, Adiwarman M, and Irvan M. Pseudo-Static Slope Stability Analysis Around the Landslide at Railway Tunnel, South Sumatera, Indonesia. *IOP Conference Series: Materials Science and Engineering*. 2019; **620**(1): 01219. DOI: http://dx.doi.org/10.1088/1757-899X/620/1/012129.

[4] Zhu HQ, Li ZH, Ma YX, and Bai ZH. Sedimentary Facies of T Structure in J Block of South Sumatra Basin, Indonesia. *Proceedings of the International Field Exploration and Development Conference 2020*. Springer Singapore, 2021: 1499-1506. DOI: https://doi.org/10.1007/978-981-16-0761-5_139.

[5] Naseer MT, and Asim S. Characterization of Shallow-Marine Reservoirs of Lower Eocene Carbonates, Pakistan: Continuous Wavelet Transforms-Based Spectral Decomposition. *Journal of Natural Gas Science and Engineering*. 2018; **56**: 629-649. DOI: https://doi.org/10.1016/j.jngse.2018.06.010.

[6] Gahana A, Sjafri I, Gani R, and Firmansyah Y. Karakterisasi Reservoir menggunakan Analisis Petrofisika pada Lapangan Y Formasi Talang Akar Cekungan Sumatera Selatan. *Padjajaran Geoscience Journal*. 2019; **3**(1): 563-571. Available from: https://jurnal.unpad.ac.id/geoscience/article/view/20839.

[7] Ginting HBR, et al. Reservoir Characterization Using Acoustic Impedance Seismic Inversion Method and Seismic Attribute in the "RST" Field of the Taranaki Basin, New Zealand. *Proceedings Indonesian Petroleum Association*; 2019. DOI: https://doi.org/10.29118/IPA19.SG.41.

[8] Kiakojury, M, Zakariaei SJ, and Riahi MA. Investigation of Petrophysical Parameters of Kangan Reservoir Formation in One of the Iran South Hydrocarbon Fields. *Open Journal of Yangtze Oil and Gas*. 2018; **3**(1): 36-56. DOI: https://doi.org/10.4236/ojogas.2018.31004.

[9] Qadri, Talha SM, Islam MA, and Shalaby MR. Application of Well Log Analysis to Estimate the Petrophysical Parameters and Evaluate the Reservoir Quality of the Lower Goru Formation, Lower Indus Basin, Pakistan. *Geomechanics and Geophysics for Geo-Energy and Geo-Resources*. 2019; **5**: 271-288. DOI: https://doi.org/10.1007/s40948-019-00112-5.

[10] Dentith M, Enkin RJ, Morris W, Adams C, & Bourne B. Petrophysics and Mineral Exploration: A Workflow for Data Analysis and A New Interpretation Framework. *Geophysical Prospecting*. 2020; **68**: 178-199. DOI: https://doi.org/10.1111/1365-2478.12882.

[11] Lis-Śledziona A. Petrophysical Rock Typing and Permeability Prediction in Tight Sandstone Reservoir. *Acta Geophysica*. 2019; **67**: 1895-1911. DOI: https://doi.org/10.1007/s11600-019-00348-5.

[12] Rifai FY, Nainggolan TB, and Manik HM. Reservoir Characterization Using Acoustic Impedance Inversion and Multi-Attribute Analysis in Nias Waters, North Sumatra. *Bulletin of the Marine Geology*. 2019; **34**(1): 380618. DOI: https://doi.org/10.32693/bomg.34.1.2019.637

[13] Rui Z, Cui K, Wang X, Lu J, Chen G, Ling K, and Patil S. A Quantitative Framework for Evaluating Unconventional Well Development. *Journal of Petroleum Science and Engineering*. 2018; **166**: 900-905. DOI: https://doi.org/10.1016/j.petrol.2018.03.090.

[14] Cox DR, Andrew MWN, and Huuse M. An Introduction to Seismic Reflection Data: Acquisition, Processing and Interpretation. Editor: Scarselli N, Adam J, Chiarella D, Roberts DG, and Bally AW. *Regional Geology and Tectonics*. Amsterdam: Elsevier; 2020: 571-603. DOI: https://doi.org/10.1016/B978-0-444-64134-2.00020-1.

[15] Alabi A and Enikanselu PA. Integrating Seismic Acoustic Impedance Inversion and Attributes for Reservoir Analysis Over 'DJ' Field, Niger Delta. *Journal of Petroleum Exploration and Production Technology*. 2019; **9**: 2487-2496. DOI: https://doi.org/10.1007/s13202-019-0720-z.

[16] Nanda and Niranjan C. *Seismic Data Interpretation and Evaluation for Hydrocarbon Exploration and Production*. Switzerland AG: Springer International Publishing; 2021.

[17] Azevedo L, Nunes R, Soares A, Neto GS, & Martins TS. Geostatistical Seismic Amplitude-Versus-Angle Inversion. *Geophysical Prospecting*. 2018; **66**(1): 116-131. DOI: https://doi.org/10.1111/1365-2478.12589.

[18] Khadem B, Saberi MR, Eslahati M, & Arbab B. Integration of Rock Physics and Seismic Inversion for Rock Typing and Flow Unit Analysis: A Case Study. *Geophysical Prospecting*. 2020; **68**(5): 1613-1632. DOI: https://doi.org/10.1111/1365-2478.12952.

[19] Maurya S, Singh N, and Singh K. *Seismic Inversion Methods: A Practical Approach*. 1st Edition. India: Springer; 2020.

[20] Abbas A, Zhu H, Anees A, and Ashraf. Integrated Seismic Interpretation, 2D Modeling Along with Petrophysical and Seismic Attribute Analysis to Decipher the Hydrocarbon Potential of Missakeswal Area. *Pakistan Journal Geology and Geophysics*. 2019; **7**(2): 1-12. DOI: https://doi.org/10.4172/2381-8719.1000455.

[21] Feng and Runhai. Estimation of Reservoir Porosity Based on Seismic Inversion Results Using Deep Learning Methods. *Journal of Natural Gas Science and Engineering*. 2020; **77**: 103270. DOI: https://doi.org/10.1016/j.jngse.2020.10327.

[22] Ali A, Alves TM, Saad F, Ullah M, Toqeer M, Hussain M. Resource Potential of Gas Reservoirs in South Pakistan and Adjacent Indian Subcontinent Revealed by Post-Stack Inversion Techniques. *Journal of Natural Gas Science and Engineering*. 2018; **49**: 41-55. DOI: https://doi.org/10.1016/j.jngse.2017.10.010.

[23] de Jonge-Anderson I, Ma J, Wu X, and Stowet D. Determining Reservoir Intervals in the Bowland Shale using Petrophysics and Rock Physics Models. *Geophysical Journal International*. 2022; **228**(1): 39-65. DOI: https://doi.org/10.1093/gji/ggab334.

[24] Hallenburg and James K. *Introduction to Geophysical Formation Evaluation*. Florida: CRC Press; 2023.

[25] Gluyas, Jon G, and Swarbrick RE. *Petroleum Geoscience*. Hoboken: John Wiley & Sons; 2021.

[26] Burger, Robert H, Sheehan AF, and Jones CH. *Introduction to Applied Geophysics: Exploring the Shallow Subsurface*. Cambridge: Cambridge University Press; 2023.

[27] Sanni and Moshood. *Petroleum Engineering: Principles, Calculations, and Workflows*. Hoboken: John Wiley & Sons; 2018.

[28] Ampilov, Yu P, Ya E, Terekhina, and Tokarev MY. Applied Aspects of different Frequency Bands of Seismic and Water Acoustic Investigations on The Shelf. *Izvestiya, Atmospheric and Oceanic Physics*. 2019; **55**: 705-720. DOI: https://doi.org/10.1134/S0001433819070028.

[29] Dondorur D. *Acquisition and Processing of Marine Seismik Data.* 1st Edition. Turkey: Elsevier; 2018.

[30] Kim Y, Hardisty R, and Marfurt KJ. Attribute Selection in Seismic Facies Classification: Application to a Gulf of Mexico 3D Seismic Survey and the Barnett Shale. *Interpretation*. 2019; **7**(3): SE281-SE297. DOI: https://doi.org/10.1190/INT-2018-0246.1.